Advanced Composite Materials
Publication details, including instructions for authors and subscription information:
http://www.tandfonline.com/loi/tacm20

Mechanical and viscoelastic properties of extruded sheets from blends containing liquid crystalline copolyesters and polycarbonate

K. Qi [a] & K. Nakayama [b]

[a] National Institute of Materials and Chemical Research, Tsukuba, Ibaraki 305-8565, Japan

[b] National Institute of Materials and Chemical Research, Tsukuba, Ibaraki 305-8565, Japan

Version of record first published: 02 Apr 2012.

To cite this article: K. Qi & K. Nakayama (1999): Mechanical and viscoelastic properties of extruded sheets from blends containing liquid crystalline copolyesters and polycarbonate, Advanced Composite Materials, 8:4, 329-343

To link to this article: http://dx.doi.org/10.1163/156855199X00317

Adv. Composite Mater., Vol. 8, No. 4, pp. 329–343 (1999)

Mechanical and viscoelastic properties of extruded sheets from blends containing liquid crystalline copolyesters and polycarbonate

K. QI and K. NAKAYAMA *

National Institute of Materials and Chemical Research, Tsukuba, Ibaraki 305-8565, Japan

Received 19 August 1998; accepted 24 September 1998

Abstract—Sheets from blends containing liquid crystalline polymer (LCP) and bisphenol-A polycarbonate (PC) were prepared using a twin screw extruder at various take-up speeds. Thermal behavior, mechanical properties, and viscoelastic properties of sheets with various compositions were investigated using differential scanning calorimetry (DSC), dynamic mechanical analysis measurement (DMTA), and sonic velocity measurement. DMTA studies showed the blends to have two glass transition temperatures (T_g) corresponding to those of the PC-rich and LCP-rich phases. Blends of PC and LCP were immiscible, although their T_gs varied slightly with composition. The dynamic and sonic moduli increased with increasing LCP content owing to the high modulus of LCP. The modulus remained unchanged with increasing LCP content at low LCP wt% (<20 wt% LCP).

Keywords: Polycarbonate (PC); thermotropic liquid crystalline polymer (LCP); immiscible blend; sheet extrusion; DMTA; DSC.

1. INTRODUCTION

Thermotropic liquid crystalline polymers (LCPs) exhibit excellent mechanical properties and high chemical stability. Over the past twenty years these properties have received considerable attention, paticularly their unusually anisotropy character, and have been the subject of recent reviews [1, 2]. An area of special interest has been the use of LCPs in isotropic polymer blends. The potential advantages of LCP properties in polymer blends is the potential to obtain fine and uniform microfibrillation of LCP with a large aspect ratio in thermoplastics due to the inherent nature of thermotropic LCPs to form elongated rod-like structures in the nematic phase during processing [3].

*To whom correspondence should be addressed.

For the purposes of improved processability and enhanced mechanical properties, paticularly the modulus and tensile strength of polycarbonate (PC), LCP is sometimes added. Blends of PC/LCP have also received wide interest in the form of various patents [4] and publications [5–15]. Properties and structure of the PC/LCP blends, such as phase behavior and morphology [5–9], rheology [5, 6], thermal behavior [8, 10], and mechanical properties [7, 11, 12] have been studied. Studies on LCP/PC ternary blends [14] and with compatibilizer [15] have also been reported.

The present investigation concerns extruded sheets of PC/LCP blends. For blend systems, it has been well demonstrated that the molecular orientation and aspect ratio of the reinforcing LCP phase may be seriously affected by processing conditions. It follows from this that the mechanical properties of the blends will also change with processing conditions.

The LCP used was a copolymer composed of 20 mol% ethylene terephthalate (PET) and 80 mol% *p*-hydroxybenzoic acid (PHB). In our study, the properties of extruded sheets of blends containing PC and LCP were studied using differential scanning calorimetry (DSC), dynamic mechanical analysis (DMTA), and sonic velocity measurement. Thermal and mechanical properties such as the sonic modulus, the glass transition temperature T_g, storage modulus E', the loss modulus E'', and the mechanical loss factor $\tan\delta$ were among the parameters included within the study. The aim of the present work was to study the connection between the properties of blends, morphological aspects, blend composition, and take-up speed of the blend.

2. EXPERIMENTAL

2.1. Materials

Commercial engineering-grade polymer LCP (Rodran LC5000, Unitika Ltd., Japan) and PC (Panlite Grade L1250, Teijin Chemical, Japan) were dried in an oven under vacuum at 80°C for 24 h and then placed in an oven at 130°C, prior to use. Pellets of these homopolymers were mixed in weight ratios of LCP/PC = 95/5, 90/10, 85/15, 80/20, 60/40, 40/60, 20/80, and 10/90.

2.2. Sheet processing

Sheets were extruded on a twin-screw lab extruder (d = 25 mm, l/d = 25, LABO PLASTOMILL, Toyoseiki Co.) through an attached coat-hanger T-die (100 mm width and 0.5 mm clearance). Temperature profiles in the barrel zones were 230, 275, 280, 285, and 288°C at the T-die. The screw rotation speed was 5 rpm for all cases and the mass output rate was approximately 9.5 g/min. Extruded sheets from the T-die were cooled in static air and rolled up using different take-up speeds (1.4, 2.3, 4.0, 10.0, 20.0 m/min) and also, on occasions, by free-dropping. PC-rich blends were easily extruded in the form of sheets and their color changed from

transparent to light yellow. LCP-rich blends were so difficult to take up in the form of sheets because they were brittle in the lateral direction and split into narrow strips.

2.3. Characterization

2.3.1. Measurement of sonic velocity. Mechanical properties of the sheets were evaluated using a sonic propagation method at room temperature with a pulse propagation meter Rheovibron DDV-5-B (Orientec Co.). The pulse frequency was 10 kHz and the pulse propagation distance between sending and receiving of the sonic pulse was 25–30 cm. The sonic modulus, $E_s = c^2\rho$, was calculated from the sonic velocity, c, and the density, ρ, of the sheet. Densities of the blend sheets were measured using a carbon tetrachloride-*n*-heptane density gradient column at 25°C.

2.3.2. Differential scanning calorimetry. Differential scanning calorimetry (DSC) experiments were performed on a Perkin-Elmer DSC-7. All experiments were carried out under a constant flow of dry nitrogen. Sample weights ranged from 20 to 30 mg and the heating rate was 20°C/min. The glass transition temperature, T_g, was taken at half the height of the heat capacity jump, and the nematic transition temperature, T_n, was defined to be the maximum of the transition peak upon heating.

2.3.3. Dynamic mechanical measurement. Dynamic mechanical thermal analysis (DMTA) of sheets was carried out on a non-resonant forced-vibration type apparatus (Model, Rheovibron DDV-II-EA, Orientec Co., Japan). DMTA was measured as a function of temperature at frequencies of 3.5, 11, 35, and 110 Hz with a heating rate of 2°C/min between −150 and 250°C. The glass transition temperature, T_g, was defined to be the maximum temperature in $\tan\delta$ and in E'' at a frequency of 11 Hz.

3. RESULTS AND DISCUSSION

3.1. Dynamic mechanical properties

For the pure PC and pure LCP, the storage modulus, E', loss modulus, E'', and mechanical loss factor, $\tan\delta$, have been presented in Fig. 1 as a function of temperature. The stepwise change in E' and accompanying changes in the E'' and $\tan\delta$ peaks indicated that there are three relaxation regions located at approximately −100, 80, and 170°C on the DMTA curve of the pure PC. These relaxations were found to be the γ_{PC}, β_{PC}, and α_{PC} relaxations, respectively, according to the discussion of Carius and others [16–18]. The glass transition temperature corresponding to the α_{PC} relaxation was somewhat higher than the T_g from the DSC result, which will be discussed later. Another relaxation, β_{PC}, indicated by the weak shoulder in $\tan\delta$ and the small step of E', is also shown as the 'intermediate' relaxation [16].

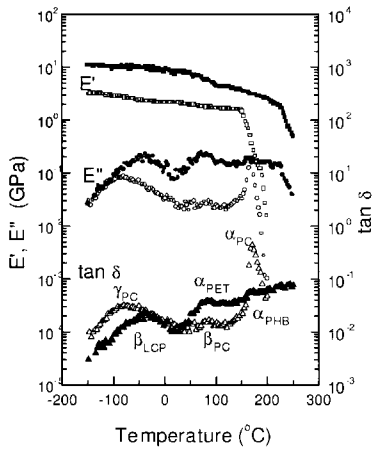

Figure 1. Temperature dependence of dynamic storage modulus E', loss modulus E'', and loss factor $\tan\delta$ for pure LCP (solid dot) and pure PC (open dot) at 11 Hz.

On the DMTA curve of pure LCP, there are two major relaxation regions located around -50 and 70°C (and extending to 80–100°C). These relaxations can be referred to as β_{LCP}, and α_{PET} relaxations, respectively, for this type of LCP, copolymer of poly(ethylene terephthalate) (PET) and poly(hydroxybenzoic acid) (PHB), according to some references [19–22]. The α_{PET} relaxation relates to the glass transition of the PET-rich phase in LCP. Another weaker peak at 160°C is attributed to the glass transition temperature of the PHB-rich phase.

DMTA for PC/LCP blends was performed in order to investigate the transition temperature of each component. DMTA results for different LCP content have been shown together in order to compare the transition temperature, with a frequency of 11 Hz. Figure 2a, b, and c shows the temperature dependence of storage modulus, E', loss modulus, E'', and mechanical loss factor, $\tan\delta$, respectively, for pure PC, pure LCP, and their blends. The relaxation processes found in the pure components were also noted in the blends. The α_{PC} peak intensity at around 170°C for the $\tan\delta$ *versus* temperature curve, which was attributed to the glass transition of the PC-rich phase, was clearly influenced by the LCP fraction. However, T_g for the PC-rich phase shifted slightly to lower temperatures by approximately 5°C for the blend with an LCP content of 90 wt%. The greater the PC contents in the blend, the higher the T_g value of the PC-rich phase. Figure 3a illustrates curves of glass transition temperature, T_g, *versus* $\tan\delta$ peak and E'' peak against LCP content, with the change of T_g with LCP being seen more clearly. Values of $\tan\delta$ at the α_{PC} peak have been plotted in Fig. 3b. The $\tan\delta$ and peak corresponding to the PC glass-rubber transition changed with LCP content to a smaller extent from 172 to 166°C and from LCP = 0 to 90%, respectively, with a decreasing $\tan\delta$ peak value corresponding to increasing LCP content.

While the glass transition α_{PET} peak of the PET phase, located close to the β_{LCP} relaxation of PC at approximately 80°C, increased in peak intensity with increasing

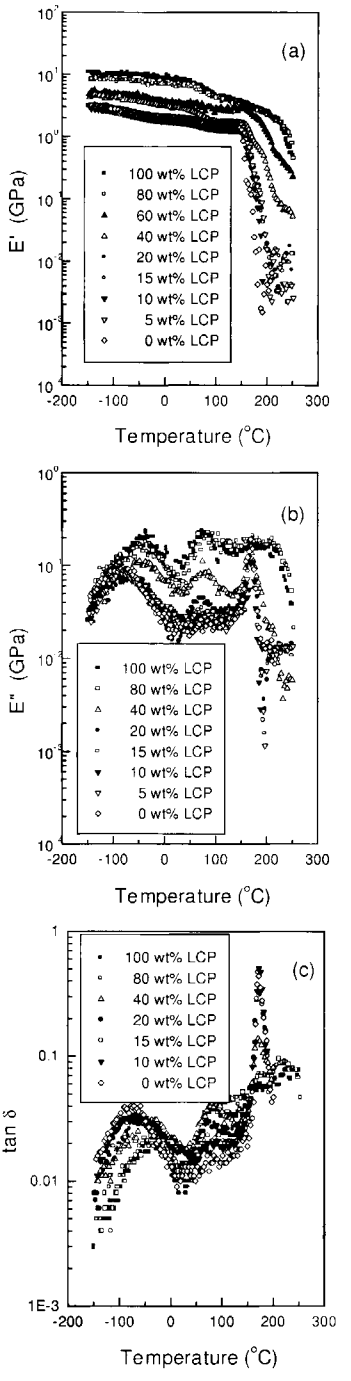

Figure 2. DMA thermogram at 11 Hz of PC/LCP blends at take-up speed of 1.4 m/min. The weight percentage of LCP is indicated. (a) dynamic storage modulus E', (b) dynamic loss modulus E'', and (c) tan δ.

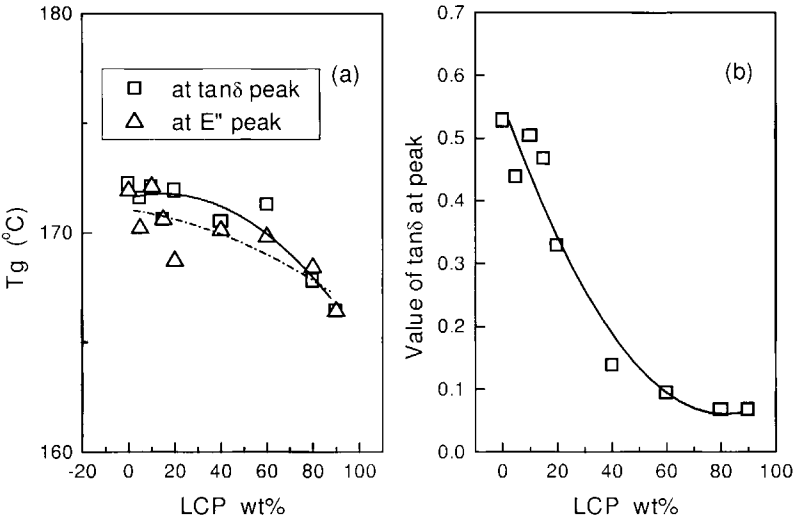

Figure 3. Changes of glass transition, α_{PC} on LCP concentrations. (a) T_g, in terms of temperature at peak of E'' and $\tan\delta$, (b) intensity, in terms of value of $\tan\delta$ at α_{PC} peak.

LCP concentration, no shift in temperature was observed with increasing LCP fraction. In the lower temperature region, γ_{PC} relaxation decreases in intensity and β_{LCP} increases in intensity with increasing LCP content. Changes in position with composition for other LCP loss peaks have not been observed.

Also, it can see that the blend moduli show a different trend in the high temperature range. For a low PC content, the blend modulus changes very slowly whereas for high PC content the modulus rapidly decreased. Such a phenomenen is related to the property of the matrix in the blends. Blend with a LCP matrix show little change in modulus above the glass temperature due to the crystalline region. However, blends with a PC matrix show a rapid change in modulus above the glass transition temperature. Thus, it can expected that phases will be inverted between the 60/40 and 20/80 LCP/PC composition blends.

From the above analysis of LCP/PC blends by DMTA, it is suggested that interactions between the PC resin molecules and LCP molecules are weak. It can therefore be postulated that immiscibility exists between these polymers in the blends, with all composition blends been separated into two regions.

For pure LCP, the structure changed significantly with drawing deformation [23] as orientation increased with increasing drawing ratio. Figure 4a and b shows DMTA of PC/LCP blends with different take-up speeds. Unfortunately, it is not possible to observe any significant change with take-up speed for both the low LCP content (20 wt% LCP) and high content (80 wt% LCP) materials.

3.2. Mechanical behavior

Mechanical properties of the PC/LCP were evaluated in terms of both dynamic modulus and sonic modulus. Figures 5 and 6 show blend modulus as a function of

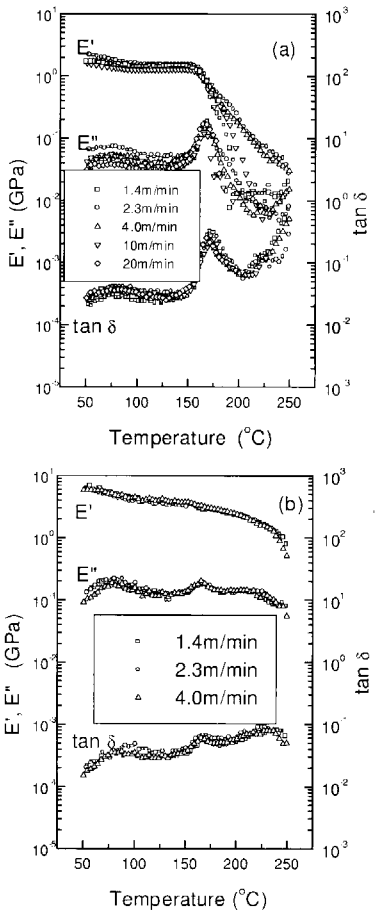

Figure 4. Dynamic storage modulus E', loss modulus E'', and $\tan\delta$ *vs.* temperature for PC/LCP. Take-up speeds are indicated. (a) 20 wt% and (b) 80 wt% LCP.

blend composition. As might be expected, the modulus increased with increasing LCP content due to the higher modulus of LCP. The measured modulus remained almost constant up to 40 wt% LCP and thereafter increased slightly. A large modulus increase was obtained for blends containing 60–80 wt% LCP. This result was similar to that obtained for PET/LCP blend systems [12].

The dependence of E' on LCP content varied with temperature, particularly for high LCP concentrations (wt% LCP = 80), as shown in Fig. 5. In Fig. 2a, the plot indicates several regions with stepwise decreases of E' due to relaxation of γ_{PC}, α_{PET}, and α_{PC}. This indicates the dependence of E' on composition to vary with temperature. It should be noted that a large decrease in E' for LCP and PC/LCP blends exists at the α_{PET} temperature. LCP exhibited a higher modulus compared to PC and acted as a dispersing phase, thus enhancing the modulus of blends at lower temperatures. At α_{PET}, glass transition of the PET results in a modulus

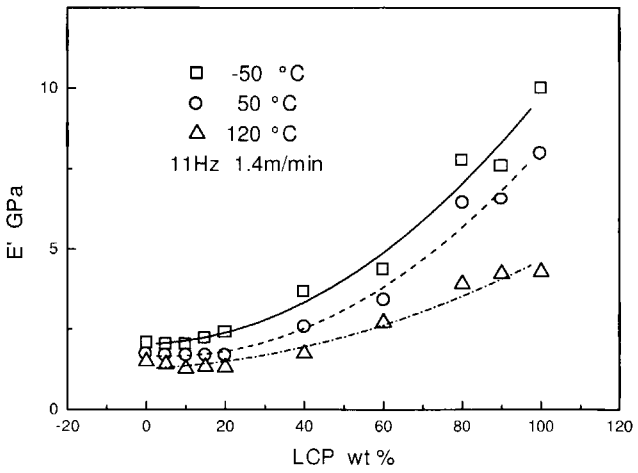

Figure 5. Composition dependence of dynamic modulus at different temperatures for PC/LCP blends. Take-up speed: 1.4 m/min, frequency: 11 Hz.

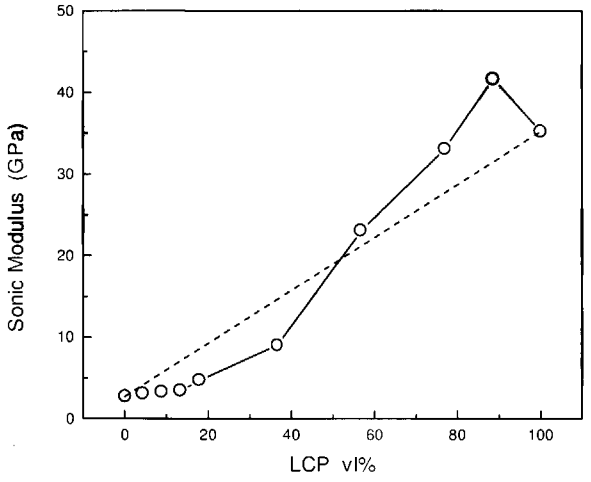

Figure 6. Sonic modulus of PC/LCP blends as function of LCP contents.

decrease, thus inverting the order of the curves for low LCP concentration. At temperatures below the glass transition of the PET component, E' increases with increasing LCP content. An inverse behavior exists above α_{PET} where the modulus decreases with increasing LCP concentration prior to the final drop connected with the transition. These phenomena clearly confirm the multiphase character of the blends. Figure 5 shows the blend modulii with 5–10 wt% LCP to be even lower than the modulus of pure PC. It can be imagined that the interface between PC and LCP components is weakly bound with poor interaction. A lower modulus in the blend when compared to the pure polymer has also been reported for several polymers such as polysulfone/LCP blends [24].

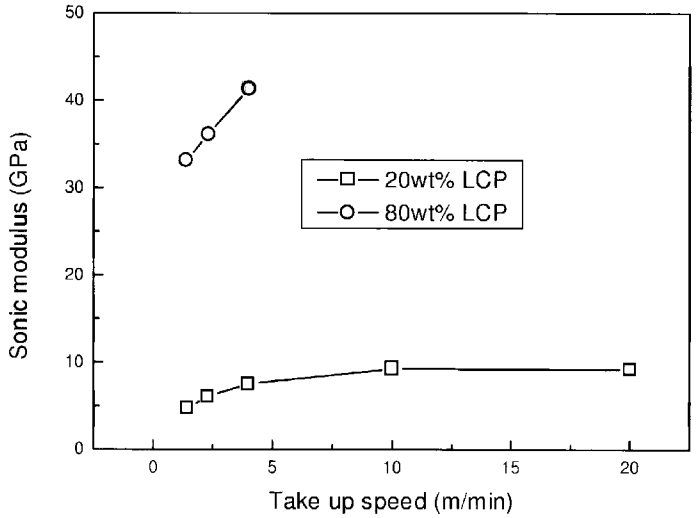

Figure 7. The sonic modulus of 20 wt% and 80 wt% LCP containing PC/LCP blends, as affected by take-up speed.

The dynamic modulus, E', remained almost constant with take-up speed of the sheets, as shown in Fig. 4a and b. However, results for sonic modulus were somewhat different. Figure 7 shows the sonic modulus of the blend containing 20 wt% LCP to increase slightly with the take-up speed while a large change exists for the blend with 80 wt% LCP. It is therefore suggested that in all blends (except for LCP > 80 wt%) the LCP phase orientation is not well developed and the fibrillation processing is not complete.

It would appear that, when the LCP content is low, the dispersed (LCP) particles are smaller and thus less deformable when stressed. At the same time, due to the low PC/LCP interfacial adhesion, slippage may occur at the interface, resulting in lower than normal drawn ratios for the LCP particles. LCP becomes a continuous matrix when increased to 80 wt% and thus is directly affected by the tensile stress during drawing.

3.3. Thermal properties

DSC curves of pure PC, LCP, and their blends have been presented in Fig. 8. The glass transition temperature, T_g, of pure PC was clearly observed in the DSC curve to be about 152°C and near the value reported in the literature. However, it was not possible to observe the glass transition temperature, T_g, of LCP in its pure state or in the blends due to their low intensity. The peak at approximately 280°C for pure LCP is attributed to the nematic transition.

It can be seen from Fig. 8 that DSC thermograms of the PC/LCP blends clearly show T_g to be close to that of pure PC. Indeed, only one T_g was detected for pure PC and PC/LCP blends. Figure 9 presents transition temperatures of the blends as

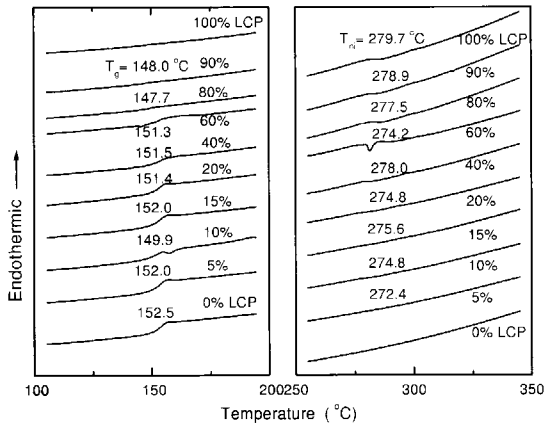

Figure 8. DSC endothermic for PC/LCP blends system at various blend compositions. The weight fractions of LCP are indicated. Note that the curve has been magnified several times, while all curves have been shifted along the axis for clarity.

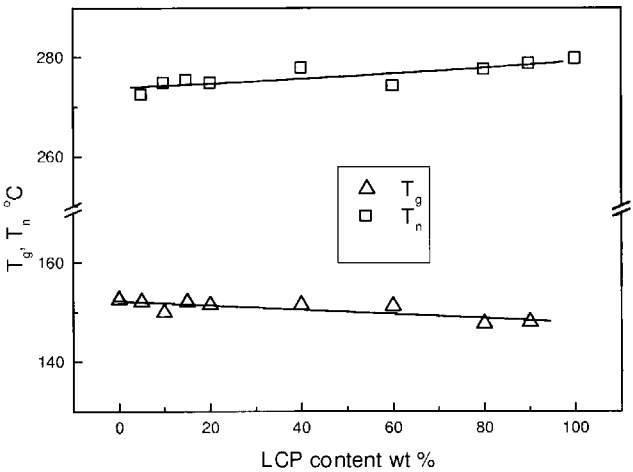

Figure 9. Variation of the transition temperature of the PC/LCP blends, T_g and T_n, with composition from DSC result.

a function of blend composition with T_g of the PC-rich phase shifting slightly to lower temperatures with increasing LCP content.

The DSC thermogams in Fig. 8 also show the melting behavior of pure LCP and the blends. In the case of pure LCP, the nematic transition temperature, T_n, was observed to be 280°C. It may also be seen that crystallization of LCP within the blends becomes progressively more difficult with increasing PC content. In fact, no endothermic peak was observed for blends containing 5 and 10% LCP, indicating that blends with a LCP content of up to 10% are entirely amorphous. The value of T_n as a function of blend composition has also been presented in Fig. 9.

In LCP/PC blends with a LCP weight fraction of greater than 90%, no peak from T_g of the PC phase is seen in the DSC traces. For LCP weight fractions less than or equal to 5%, the T_n peak is not present and only T_g for PC is observed. In the blends with LCP weight fractions between 5% and 90%, both T_g for PC and T_n for LCP appear in the DSC thermograms.

Figure 9 shows more clearly the dependency of the sheet T_n and T_g on the LCP content. Peak shapes for melting of LCP and the glass transition shape for PC did not change significantly with LCP content. T_g for PC resin shifted to a lower temperature and T_n increased slightly, respectively, with increasing LCP content as can be seen in Fig. 9. The invariance of T_n indicates the LCP-rich nematic phase to be nearly free of PC molecules for all weight fractions. This indicates qualitatively that the blends were separated into phases of an almost pure LCP phase together with a PC-rich phase that contained a significant number of LCP molecules. Thus, interactions between the PC molecules and the LCP molecules are suggested to be weak so that and the blends separate into two regions. The authors are currently unable to explain the downward trend in the PC-rich T_g for large weight values. The implication is that the solubility of LCP chains in PC increases for weight fractions larger than 70%.

Previous research [25] has suggested LCP to be miscible in PC for small weight fraction, but features both nematic and isotropic phases for large fractions of LCP.

Figure 10a and b shows DSC heating curves for different take-up speeds. Peak shapes, in addition to the transition temperature (Fig. 11) were not significantly affected by the take-up speed. In PC-rich blends (20 wt% LCP) the PC resin glass transition was found to be almost independent of the take-up speed, whereas T_n changed slightly, as shown in Fig. 10a. On the other hand, for LCP-rich blends (80 wt%) shown in Fig. 10b, the PC glass transition and LCP isotropic temperature varied with take-up speed. This phenomenon suggests elongation (different take-up speed) to have a larger effect on LCP than on PC.

3.4. Rheological behavior

Extrusion torque and pressure of the LCP/PC blends as a function of LCP content are shown in Fig. 12. Torque and pressure are clearly observed to decrease monotonically with increasing LCP content, as expected. The torque falls rapidly with increasing LCP content up to 5 wt%, and then levels off with further LCP increase.

Such a significant torque and pressure decrease could be attributed to the orientation of LCP in the melt state. However, for PC/LCP blends sheets, mechanical properties are very low and also appear to be independent of the take-up speed as noted earlier. There seems to be no obvious evidence of LCP orientation in the PC/LCP blends or else chain orientation is not fully developed. Considering the extrusion processing of PC/LCP, almost all of the deformation occurred on the 'melt part' of the sheet shortly after emerging from the T-die. The increase in take-up speed only affects the melt drawing (there is a melt drawing processing). Chain

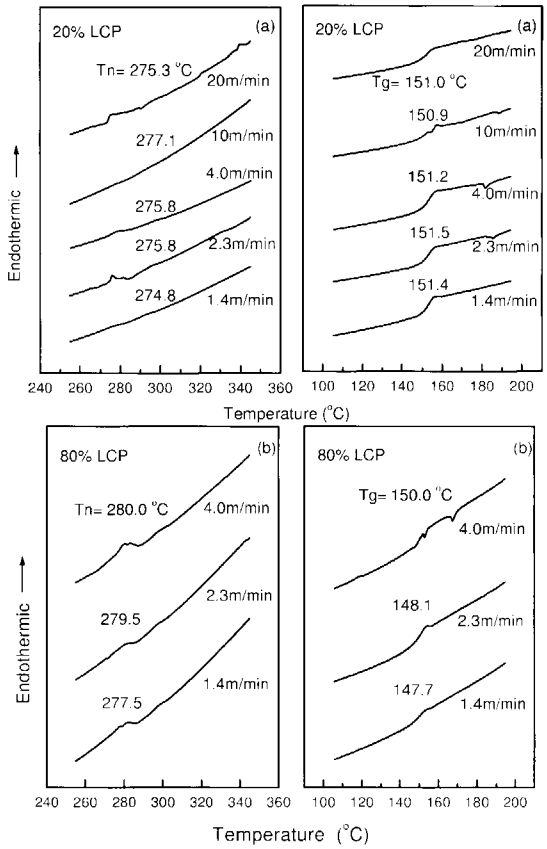

Figure 10. DSC thermograms of the PC/LCP blends of different take-up speeds. LCP weight percent: (a) 20%, (b) 80%.

extension in the liquid state can always occur in the flow field. The viscosity is reduced significantly by only a small amount of LCP. However, for the sheet product, extended chains can only be expected when cooling, as well as other conditions, are suitable to 'freeze in' the chains.

In general, many parameters need to be considered regarding the conditions under which the extended chains will be preserved, e.g. nature of the flow field, strain rate, strain, and temperature of the extrusion process. So far, the details of controlling LCP fibrillation are not well understood. In other words, the conditions required for fibrillation of LCP domains have not been clearly established. Regarding extrusion, the application of strong extensional flows is essential for the formation of LCP fibers [26]. Work on injection molding [14, 27] has shown a skin-core distribution of LCP microfibrils to be induced in the matrix due to the high shear rate, i.e. injection shear rates in the range of $10^3 - 10^5$ s^{-1}, and higher than it occurs in extrusion. It is difficult to say whether shear stress or elongation stress (in the case of extrusion and take-up) is more favourable regarding fibrillation formation. However, it is

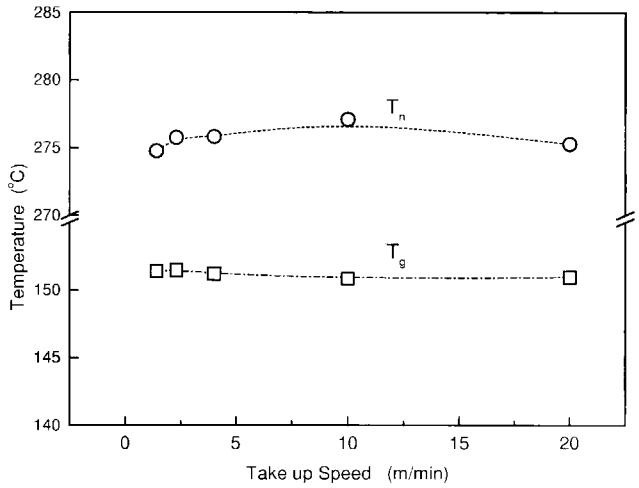

Figure 11. The transition temperature of 20% LCP containing PC/LCP blend, as affected by take-up speed.

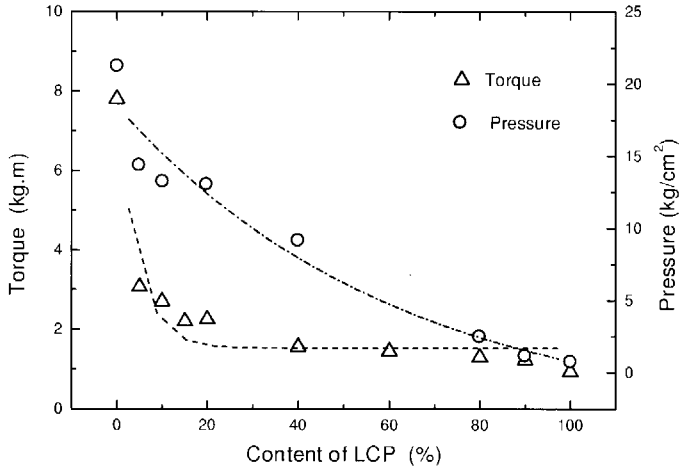

Figure 12. Variation of torque and pressure during extrusion of PC/LCP blends with different LCP content.

generally recognized that the degree of LCP fibrillation strongly depends on the processing conditions. Spherical LCP droplets, instead of fibrils, often result from poor processing control.

The main point of note is that the torque and pressure of blends decreased significantly when a small amount of LCP was added to the PC polymer. This is a very important phenomenon as it implies better improved processibility of the LCP/PC blends due to the reduced viscosity. If, for the purpose of processing, LCP serves as a processing aid for injection molding or extrusion, then usage of less than 5 wt% of LCP is sufficient. However, if the aim is to improve mechanical

properties of the LCP blends, i.e. for the purpose of forming *in situ* fibrils to reinforce thermoplastics, then at least 40 wt% of LCP is necessary.

4. CONCLUSIONS

(1) The T_g of PC and T_n (nametic transition temperature) of LCP were observed in both the pure state and blends by DSC. T_g of the PC-rich phase was slightly shifted to lower temperatures with increasing LCP content. In blends, the DSC curves showed separate transition temperatures for PC and LCP. These DSC results, together with DMTA data, indicate poor miscibility between PC and LCP.

(2) The torque and pressure decreased monotonically with increasing LCP content. The torque fell rapidly with increasing LCP content up to 5 wt% and then levelled off with further increases. For the purpose of processing, 5 wt% of LCP is sufficient, whereas at least 40 wt% is required for use as reinforcement.

(3) DMTA and DSC curves were not significantly affected by the take-up speed. However, the sonic modulus changed for blends with higher percentages of LCP. At the present time, it is not possible to provide definite answers to the question of whether PC/LCP blends are affected by the take-up speed.

REFERENCES

1. O. Roetting and G. Hinrichsen, *Adv. Polym. Technol.* **13** (1), 57 (1994).
2. D. Dutta, H. Fruitwala, A. Kohli and R. A. Weiss, *Polym. Eng. Sci.* **30**, 1005 (1990).
3. W. Brostow, *Polymer* **31**, 779 (1990).
4. L. A. Utracki, *Polym. Eng. Sci.* **35** (1), 2 (1995).
5. S. Lee, P. T. Mather and D. S. Pearson, *J. Appl. Polym. Sci.* **59** (2), 243–250 (1996).
6. W. Brostow, T. Sterzynski and S. Triouleyre, *Polymer* **37** (9), 1561–1574 (1996).
7. K. A. Khan, R. Kahraman, E. Z. Hamad, S. Ali and S. H. Hamid, *J. Appl. Polym. Sci.* **64** (4), 645–652 (1997).
8. H. S. Lee, W. H. Jung and W. N. Kim, *Polym. Bull. (Berlin)* **37** (4), 503–510 (1996).
9. D. Winerich, A. Siegmann and M. Narkis, *J. Macromol. Sci., Phys.* **36** (2), 247–262 (1997).
10. C. L. Choy, K. W. F. Lau, Y. W. Wong, H. M. Ma and A. F. Yee, *Polym. Eng. Sci.* **36** (6), 827–834 (1996).
11. F. P. La Mantia, A. Roggero, U. Pedretti and P. L. Magagnini, Liquid-crystalline polymer systems, *ACS Symp. Ser.* **632**, 110–117 (1996).
12. D. Beery, S. Kenig, A. Siegmann and M. Narkis, *Polym. Eng. Sci.* **36** (2), 229–236 (1996).
13. M. Roemer and A. Neupauer, *Kunststoffe* **86** (9), 1310, 1312, 1315–1316 (1996).
14. Q. Xu, Y. Leng and Y. W. Mai, *Polym. Eng. Sci.* **36** (6), 769–777 (1996).
15. D. Dutta, R. A. Weiss and J. He, *Polymer* **37** (3), 429–435 (1996).
16. H. Carius, A. Schonhals, D. Guigner, T. Sterzynski and W. Brostow, *Macromolecules* **29** (14), 5017 (1996).
17. J. Y. Jho and A. F. Yee, *Macromolecules* **24**, 1905 (1991).
18. F. Weigand and H. W. Spiess, *Macromolecules* **28**, 6361 (1995).
19. U. W. Gedde, D. Buerger and R. H. Boyd, *Macromolecules* **20**, 988 (1987).

20. W. Brostow and D. Samatowicz, *Polym. Eng. Sci.* **33**, 581 (1993).
21. D. Chen and H. G. Zachmann, *Polymer* **32**, 1612 (1991).
22. D. Y. Yoon, N. Maschiochi, L. E. Depero, C. Viney and W. Parrish, *Macromolecules* **23**, 1793 (1990).
23. A. Kaito, M. Kyotani and K. Nakayama, *J. Macromol. Sci.-Phys.* **B34** (1, 2), 105–118 (1995).
24. V. G. Kulichikhin, O. V. Vasil'eva, I. A. Litvinov, E. M. Antipov, I. L. Parsamyan and N. A. Plate, *Journal of Appl. Polym. Sci.* **42**, 363 (1991).
25. H. G. Schild, E. S. Kolb, R. A. Gaudiana, Y. Chiang and W. C. Schwarzel, *J. Appl. Polym. Sci.* **46**, 959 (1992).
26. M. F. Champagne, M. M. Domoulin, L. A. Utracki and J. P. Szabo, *Polym. Eng. Sci.* **36** (12), 1636 (1996).
27. D. Beery, S. Kenig and A. Siegmann, *Polym. Eng. Sci.* **31**, 451 (1991).